

DEVELOPMENT AND OPTIMISATION OF RESTING STATE fMRI IN THE MOUSE BRAIN AT 9.4T

Arun Niranjani¹, Jack A. Wells¹, and Mark F. Lythgoe¹

¹Centre for Advanced Biomedical Imaging, University College London, London, United Kingdom

Target Audience: Researchers in the fields of preclinical imaging, resting state fMRI, mouse brain fMRI, mouse models of neurological diseases.

Purpose: Functional connectivity is defined as the network of temporal links between the neuronal activities of spatially distinct brain regions, and is believed to be affected by many neurological diseases such as Alzheimer's Disease and Multiple Sclerosis¹. Application of resting state methods to mouse models of neurological diseases provides a platform for the investigation of functional connectivity abnormalities in pathology under experimentally controlled conditions. Functional connectivity Magnetic Resonance Imaging (fcMRI) has only recently been applied to the mouse brain in the resting state²⁻⁴. The aim of this work is to develop an optimised experimental protocol for acquiring resting state fcMRI data from the mouse brain, with a semi-automatic pipeline for image processing and higher-level analysis. There are significant experimental challenges when applying fcMRI to the mouse brain: balancing spatial resolution against temporal stability; limiting susceptibility induced image artefacts; preserving neurovascular coupling and BOLD contrast whilst maintaining sufficient anaesthesia; and minimising head motion.

Methods: An Agilent 9.4T MRI scanner was used in conjunction with a Rapid 4 channel mouse brain surface coil. Experiment 1 investigated the relationship between the temporal stability of GE-EPI measurements and image resolution. We performed GE-EPI experiments on an agar phantom with multiple field of views (FOVs) and matrix sizes (12 axial slices, slice thickness of 0.5 mm, slice gap of 0.1 mm, TR = 2 s, TE = 19 ms). Once a set of suitable parameters was obtained, they were applied *in vivo*. Experiment 2 focussed on removing susceptibility artefacts caused by inhomogeneities in the magnetic field within the volume enclosed by the surface coil. This *in vivo* pilot study (N=1) tested the use of an agarose cap placed on the mouse head⁵ to minimise image distortion. In experiment 3, we applied our experimental protocol to obtain resting state data (N=1). Induction and animal preparation was conducted using 2% isoflurane, and then switched to medetomidine for data acquisition (mass dependent dose of 0.04 mg/kg for an initial bolus, 0.08 mg/kg/hr for constant infusion⁵). The animal was continuously maintained on a gas mixture of 0.1L/min O₂ and 0.4 L/min of medical air. This anaesthetic protocol yielded reproducible anaesthesia with an average respiration rate of approximately 120 breaths per minute. A custom *in vivo* mouse head holder has been created using 3D printing, in order to minimise head motion. The reduction in head motion through the use of medetomidine (which induces light, rapid breathing) and the head holder was evaluated by visual inspection of the GE-EPI sequences. Experiment 4 was a preliminary *in vivo* study (N=3) to inform further development of the image processing and analysis pipeline. Currently the pipeline consists of the following: brain masking; image re-alignment; spatial smoothing; linear and quadratic detrending; temporal filtering; slice timing corrections; seed voxel correlation analysis; group independent component analysis (ICA) using the GIFT Toolbox⁶.

Results: GE-EPI temporal stability was investigated in an agarose phantom. At a smaller FOV (25 mm x 25 mm), significant temporal instability was found (tSNR = 2.4), shown in the mean GE-EPI signal plots in Fig 1. A matrix size of 96 x 96 with a FOV of 30 mm x 30 mm was found to yield a stable signal (tSNR = 192). We employed the use of an agarose cap to reduce susceptibility artefacts (Fig 2 red arrow). The improvement of image quality can be clearly seen in Fig 2. Subsequently we used a GE-EPI sequence to acquire *in vivo* resting state data. Fig 3 demonstrates the improvement in BOLD data following the application of the processing pipeline. Fig 4 shows a preliminary result from ICA (fixed at 20 components) of a single subject with 6 resting state scans; each scan consisting of 150 timepoints. Bilateral cortical activation can be seen in a single component following global signal regression.

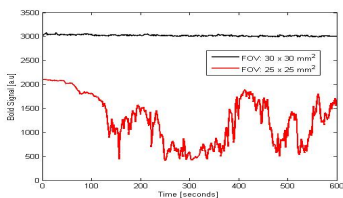


Fig 1. Temporal instability in an agar phantom at FOV = 25 mm x 25 mm.

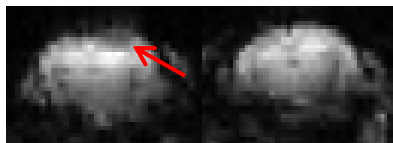


Fig 2. Application of an agar cap to the mouse brain (right) reduces susceptibility artefacts.

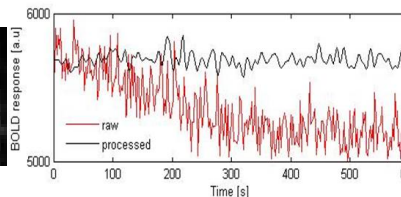


Fig 3. Raw and processed BOLD timecourses from one voxel in the mouse brain *in vivo*.

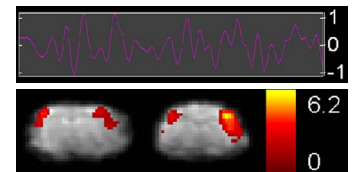


Fig 4. A bilateral component derived using ICA. The timecourse is scaled by percentage fluctuation; the heat map is scaled by z-score.

Discussion: We have addressed each of the fcMRI major issues previously highlighted. Temporal stability has been improved by optimising the field of view, anaesthetics, and minimising head motion using a custom-built *in vivo* mouse head holder, to maximise sensitivity to resting state BOLD fluctuations. We have reduced susceptibility artefacts using a site-specific agarose cap to reduce distortion, which may be further improved with the application of voxel shift maps derived from B₀ images⁷. We have implemented our pipeline to improve the quality of the *in vivo* data and apply ICA to detect bilateral cortical activation. Future work includes investigating effects of image normalisation and whole-brain signal regression. Linear regression of confounding variables such as respiration and motion estimates will be characterised and incorporated into the analysis pipeline. In this work we are developing a much needed framework for resting state fcMRI in mice, to enable assessment of temporal links of regional neuronal activity in the mouse brain for future application to genetic models of neurodegenerative disease.

References: [1]. van den Heuvel, M.P. and H.E. Hulshoff Pol, *Eur Neuropsychopharmacol*, 2010. **20**(8): p. 519-34. [2]. Jonckers, E., et al., *PLoS One*, 2011. **6**(4): p. e18876. [3]. Guilfoyle, D.N., et al., *J Neurosci Methods*, 2013. **214**(2): p. 144-8. [4]. Little, D.M., et al., *Journal of Alzheimer's Disease*, 2012. **32**(1): p. 101-107. [5]. Adamczak, J.M., et al., *Neuroimage*, 2010. **51**(2): p. 704-712. [6] <http://mialab.mrm.org/software/gift/index.html>. [7] Jezzard, P., Balaban, R.S., *MRM*, 1995; **34**: p. 65-73.